

Towards Causal Relationship in Indefinite Data: Baseline Model and New Datasets

Hang Chen, *Xinyu Yang*, Keqing Du

Abstract—Integrating deep learning and causal discovery has encouraged us to spot that learning causal structures and representations in dialogue and video is full of challenges. We defined These data forms as “Indefinite Data”, characterized by multi-structure data and multi-value representations. Unlike existing adaptable data forms, Indefinite Data still faces gaps in datasets and methods. To address the dataset gap, we release two high-quality datasets - *Causalogue* and *Causaction*, containing text dialogue samples and video action samples with causal annotations respectively. Moreover, the method gap arises from the coexistence of multi-structure data and multi-value representations, breaking the assumptions of all current methods, rendering them infeasible on Indefinite Data. To this end, we propose a probabilistic framework as a baseline, incorporating three designed highlights for this gap: 1) establishing Causation Condition of representations using the independence of noise terms under non-fixed causal structures, 2) treating causal strength as a latent variable and measuring the reconstruction loss in the correlation space, and 3) estimating the effects of latent confounders. These highpoints make the probabilistic model capable of overcoming challenges brought by the coexistence of multi-structure data and multi-value representations, and pave the way for the extension of latent confounders. Comprehensive experiments have evaluated baseline results of causal structures, causal representations, and confounding disentanglement. Our codes are available at [Github](#) (click here).

Index Terms—Causal Data, Causal Representation, Causal Structures, Datasets, Baseline Model

I. INTRODUCTION

In light of the recent advances in deep learning, there is a growing tendency to incorporate causal discovery in more complex forms of data, including images [1], [2], text [3], and videos [4]. Generally, there are two purposes for these incorporations: one is to uncover the underlying **causal structure** [5]–[9] within the data, the other is to learn effective **causal representations** [10]–[15].

Our recent work [16] has summarized different forms of these incorporations based on causal structure and causal representation respectively. Regarding causal structure, there are **single-structure** data [17]–[19] and **multi-structure** data [20]–[22], depending on whether multiple causal structures (causal graphs) are involved in the dataset or task. For example, fMRI dataset [23] suggests the different brain region activity levels of Patient *A* and *B*, corresponding to two causal structures. Concerning causal representation, there are **single-value** representations [24]–[26] and **multi-value** representations [27]–[29], depending on whether the causal variables

need to be transformed into deep representations. Variables like age, height, weight, blood pressure are typically treated as single-value representations [30], while a sentence [31] or a video [32] often needs to be converted by deep models into multi-value representations (such as sentence embeddings or optical flows) to make them calculable.

Our work [16] further conjectured the emergence of a new causal data paradigm - **Indefinite Data** with the characteristics of both **multi-structure** data and **multi-value** representations. For instance, taking any dialogue as an input, could we recover the complete causal relationships between utterances and learn each utterance’s causal representation? Or, if we replace the dialogue with a video, could we learn the internal relationships among segments and their corresponding causal representations?

Despite the comprehensive definition provided by [16], the study of Indefinite Data still faces two research gaps: the **dataset gap** and the **method gap**. Specifically, causal relationships in dialogues and videos are often obscure and subjective, making it challenging to collect samples with obvious causal relationships and objective annotations. Moreover, the co-occurrence of multi-structure data and multi-value representations breaks the hypotheses of all existing methods, resulting in their poor adaptability to Indefinite Data.

To overcome these research gaps, we aim to release two high-quality Indefinite Datasets and a baseline model, specifically:

In Section 3, we analyze the causes of the dataset gap and particularly the method gap. Existing works on multi-value representations rely on a strong hypothesis that the causal structure is fixed and known [33]–[35]. Therefore, each causal variable can receive information from accurate parent set. Similarly, studies on multi-structure data operate under the hypothesis of single-value representations [36]–[38], in which the precision of single-value representations provides indispensable statistical strength (e.g., reconstruction error [20] or variations in distribution [22]) for identifying multiple structures’ invariances and dynamics. However, the co-occurrence of multi-value representations and multi-structure data breaks the fundamental hypotheses of these two mainstream methods, necessitating a redesign of how causal representations can be learned and how new causal structures can be adapted.

In Section 4, we proposed a probabilistic framework as a baseline model based on Structural Causal Models (SCMs), featuring three novel designs: 1) The incorporation of an independent noise representation enables the output representation to discern specific causal relationships, thus completing the conversion from deep representations to causal representations.

The authors are with the Department of Computer Science and Technology, Xi’an Jiaotong University, Xi’an Shannxi, 710049.
E-mail: albert2123@stu.xjtu.edu.cn, yxyphd@mail.xjtu.edu.cn, dukeqing@stu.xjtu.edu.cn

2) Treating the causal strength, rather than the noise term, as a latent variable avoids conflicts arising from different causal structure distributions. 3) The estimation of confounding effects disentangle the causal representation and the confounding representation, making the model enable to adapt to data with latent confounders.

In Section 5, we introduced two brand-new Indefinite datasets - *Causalogue* and *Causaction*. *Causalogue* is a text dataset containing dialogue samples used for analyzing causal relationships between utterances. To ensure the causal relationships are apparent and objective, we utilized GPT-4 to generate dialogues according to pre-defined causal rules. *Causaction* is a video dataset containing different action segments, used for analyzing the causal relationships between different actions within a video. Annotators were asked to judge causal relationships directly based on low-level labels, rather than judging each video sample, thereby significantly reducing the subjectivity of causal relationships.

In Section 6, we designed comprehensive evaluation metrics for Indefinite data on causal representation and causal structures, and compared them with some of the most adaptable SOTA methods. Additionally, to directly evaluate the performance of deconfounding, we also created a synthetic dataset with a known confounding distribution.

In summary, for Indefinite Data, this paper provides why the gaps arise, what the baseline model looks like, how the high-quality datasets be created, and which evaluations should be concerned. Together with the basic definitions already proposed in our previous work [16], it sets a promising onset for causal research in such causal data with fewer constraints and forms closer to the real world.

II. PRELIMINARIES

Definition 1 (Causal representation). *The causal representation \hat{X} represents the computed values of causal variables when constructing a causal model. Causal representations should meet the following two conditions:*

- *Correlation Condition: For any two causal variables that exist correlation relationship, their corresponding causal representations should contain the information of correlation.*
- *Causation Condition: For any two causal variables that exist causal relationship, their causal representations should contain the information about the causal relationship.*

For example, paper [39] proposed that graph classification satisfies the SCM-based causal structure: $Y \leftarrow C \leftarrow G \rightarrow B$, where G represents the observed graph, C signifies the causal pattern, B stands for the background pattern, and Y represents the label. If \hat{C} , \hat{G} , and \hat{B} correspond to the three causal representations of C , G , and B , there are no causal relationships but correlations between C and B . As such, the value of $\text{cossim}(\hat{C}, \hat{B})$ is close to 1 (Correlation Condition). Furthermore, \hat{C} and \hat{B} should also meet the Causation Condition: for all samples satisfying this causal structure, the prediction results of the classifier should not change when \hat{C} is combined with a set of \hat{B} from different samples.

TABLE I
EXAMPLES ABOUT CAUSAL VARIABLES AND REPRESENTATION

Category	Variables	Deep model	Representation	Dimension(D)
Single-value	Age	-	25 (1-dimension value)	D=1
	Voltage	-	2 (1-dimension value)	D=1
Multi-value	Token	RoBERTa	tensor	D=768, 1024
	An image	LeNet-5	5*5-dimension tensor	D=5*5

We use D to represent the dimensions of representation (i.e., $\hat{X} \in \mathbb{R}^{N \times D}$, where N represents the number of causal variables) and there are two types of causal representations:

Single-value Representation (D = 1): This type of variable inherently exists in numerical form, and thus, there is no necessity for the use of deep representation.

Multi-Value Representation (D > 1): This type of variable doesn't inherently exist in numerical form and must be transformed into deep representations to enable computations.

Table I reveals the fundamental distinction between single-value and multi-value representations. Single-value representations are static, while multi-value representations are dynamic (i.e., less precise). Thus, single-value variables often employ various statistical advantages to recover causal structure, such as independence testing and independent component analysis (ICA), while multi-value representation can only rely on approximate correlation estimates, such as similarity and divergence.

Definition 2 (Causal structure). *The causal structure \mathcal{G} , represented as a causal graph w.r.t. Directed Acyclic Graph (DAG), is used to describe a set of causal relationships.*

Many existing works [21], [22], [40] involved with multi-structure data demonstrate significantly different approaches compared to those associated with a single-structure data. Hence, we use M to represent the number of structures and introduce two types of causal structures:

Single-structure Data (M = 1): For a given dataset or task, there exists only a single causal graph \mathcal{G} , indicating a fixed causal structure.

Multi-structure Data (M > 1): For a given dataset, multiple causal graph $\{\mathcal{G}\}_{m=1}^M$ exist, implying a not unique causal structure for each sample.

The difference between single-structure and multi-structure data lies in the fact that if a single-structure method is directly applied to multi-structured data, a new model needs to be refitted whenever a new causal structure is analyzed.

Moreover, from above basic definitions, the definition of Indefinite Data is as following:

Definition 3 (Indefinite Data). *The causal relationships exist in a dataset $\mathbf{D} = \{X_s\}_{s=1}^S$ which has S samples and M ($M > 1$) causal structures ($\mathcal{G} = \{\mathcal{E}_m, \mathcal{V}_m\}_{m=1}^M$). Each structure \mathcal{G}_m corresponds to several samples separately. Hence, each sample $X_{s,m} \in \mathbb{R}^{N_m \times D}$ ($D > 1$) belongs to an individual causal structure $\mathcal{G}_m = \{\mathcal{E}_m, \mathcal{V}_m\}$ and consists of N_m variables: $X_s = \{x_{s,m,n}\}_{n=1}^{N_m}$. $\hat{x}_{s,m,n} \in \mathbb{R}^{1 \times D}$ represents the causal representation of a variable $x_{s,m,n}$.*

Example 1 (Indefinite Data). *IEM Dataset [41] is a conversation dataset with each sample including a dialogue between*

two speakers. All 100 samples are assigned into 26 structures based on the speaker identifies and turns. Each sample consists of 5-24 causal variables where each variable is an utterance represented by word embeddings.

Moreover, given the major examples of Indefinite Data involves textual conversations and video sources, we propose a hypothesis about the causal identifiability:

Hypothesis 1 (Causal Identifiability). *The natural order (e.g., time-order) w.r.t. $\{x_{s,m,n}\}_{n_m=1}^{N_m}$ is defined as a linear order $\prec_{X_{s,m}}$. Given that causal order w.r.t. $\{x_{s,m,n}\}_{n_m=1}^{N_m}$ is defined as a partial order $\preceq_{X_{s,m}}$, $\forall \langle x_1, x_2 \rangle \in \prec_{X_{s,m}}$ (i.e., $x_1 \prec_{X_{s,m}} x_2$), there must be $\langle x_1, x_2 \rangle \in \preceq_{X_{s,m}}$.*

Hypothesis 1 illustrates the natural linear order of Indefinite data (e.g., $\{U_1, U_2, U_3, U_4\}$, where U_1 to U_4 respectively represent 4 utterances appearing in time-series, and $U_i \prec U_j$ indicates that U_i precedes U_j in time) belongs to the causal partial order. Consequently, the adjacency matrix of the natural linear order is a triangular matrix, which naturally corresponds to a DAG. Thus, there is no need for measures such as acyclic constraints [42] to ensure causal identifiability.

III. RESEARCH GAPS OF INDEFINITE DATA

A. Related Work

1) *Multi-value Representation & Single-structure Data:* In the domain of images, [43] initially treats object features and context features as two causal representations, learning via the integration of additive noise models (ANMs) and neural networks. Subsequent works followed this pathway and developed various methods to extract causal representations, such as LSTM [29] and linear layers [44], [45], along with more refined causal variables [33]–[35].

As for text, existing studies, based on prior knowledge, pre-set that certain words carry essential causal clues or interferences at the word-level embedding, such as verbs [46], conjunctions [47], and terminologies [48]. For utterance-level embeddings, the SCM is often used as guiding prior knowledge, spurring a vast amount of work on the generation of exogenous latent causes [31], [49].

In other fields, like audio or graph, decoupling at the representation level often occurs [39], [50], [51]. This results in splitting the representation into a set of variables that have causal relationships with labels, and another series of variables exhibiting spurious correlation with labels.

2) *Multi-structure Data & Single-value Representation:* A main body of work refers to methods for addressing such data as amortized learning or mixed models learning [20]–[22], exploring the linear mixed effects models [52], multiple amortized structures [21], [40], and across samples learning [53]–[55]. The range of approaches to multi-structure data relevant to single-value representation including [22] who utilizes the reconstruction error $loss(X, \hat{X})$ to control the distribution of causal strength, concurrent work find the invariable causal relationship across structures via statistics of single-value representation [40], [52].

B. Method Gap

Indefinite Data ($D > 1$ & $M > 1$) can be simply considered as an integration of two types of $D = 1$ & $M > 1$ and $M = 1$ & $D > 1$. However, the two types both rely on the hypothesis that the other dimension is $= 1$.

When we aim to design a model to learn multi-value causal representations, the infer process always inspired by fixed, prior-regarded causal structures. Formally, we assume $\hat{X} = infer(X)$, where $infer(\cdot)$ is designed through a fixed causal structure. For instance, [39] believe that the background B of a graph G could mislead the labels Y caused by causal pattern C , due to a fork structure on the path between B and Y , as $Y \leftarrow C \leftarrow G \rightarrow B$. the Causation Condition of the causal representation should be satisfied as: $\hat{X} = infer(P(Y|do(C)))$. It describes that the strength of the causal pattern C to the Y should remain unchanged with replacing any B from other samples. Alternatively, when we discover that spatial features have created front-door paths to the label, the Causation Condition should be equal to the what an intermediate variable X^* satisfies [34], which reads: $\hat{X} = infer(P(Y|X^*))$. In summary, if we break the hypothesis of single-structure data, there is a lack of causal clue to formulate the Causation Condition.

Similarly, when we wish to learn some invariants from multi-structure data, some unchanged causal relationships can be uncovered from single-value representations. That is, $G = infer(X)$, where $infer(\cdot)$ is designed through single-value representation. For example, [40] proposed $G = infer(\{p(X_m)\}_{m=1}^M)$ to decouple different structural distributions relying on the accurate statistics value of single-value representation. Furthermore, the reconstruction loss of a single-value representation, written as $G = infer(loss_{rc}(X, \hat{X}))$, also theoretically supports the ELBO of the posterior distribution of causal strengths [22]. This is not achievable in multi-value representations, as X only satisfies the Correlation Condition, while \hat{X} satisfies the Causation Condition.

Taking deep model as an instance, p_φ and q_θ represents the encoder and decoder of generative model from domain of causal variable X to the domain of causal representation \hat{X} where f_i is causal strength responsible for the causal mechanism.

M = 1 & D = 1: The causal strength can be estimated by the statistical strength observable in the samples.

M > 1 & D = 1: We can separate the problem to several tasks of single-structure data. Reconstruction loss amounts to $\{f_m\}_{m=1}^M$, where can be regarded as a multi-task optimization problem, $\alpha_1 f_1 + \alpha_2 f_2 + \dots + \alpha_M f_M$, where α_m is the weights of the sample quantity per structure.

M = 1 & D > 1: The reconstruction loss can be written as: $p_\varphi \circ f \circ q_\theta$, where f represents the determined part due to fixed causal structure.

M > 1 & D > 1: We are only able to attain an approximate $\tilde{p}_\varphi = p_\varphi \circ f_m$, which results in a final reconstruction loss of $\tilde{p}_\varphi \circ q_\theta$. Causal strength f_m comprises an undetermined part.

C. Dataset Gap

In our previous work [16], we collected a set of public datasets satisfying the requirements of Indefinite Data. The limitations mainly arise from the fact that Indefinite Data largely exists in continuous forms, making the demarcation of causal variable boundaries a significant challenge. For instance, in the arithmetic datasets [56]–[58], although much effort has been devoted to discover the relationships between different steps, the non-uniqueness of the reasoning process makes it difficult to transcribe the chains of thought (CoT) into a set of causal variables. However, video and dialogue datasets do have clear variable boundaries; for example, video datasets [59], [60] can be segmented based on action semantics, and each utterance in dialogue datasets is discrete [41], [61]. However, on these datasets, most causal relationships are obscure, which leads to poor consistency in manual annotation. Taking dialogue as an example, utterances that have not been observed before might likely act as confounding factors influencing the correlation between observed utterances. Moreover, the standards for judging whether there is a causal relationship between two utterances is terribly subjective. Up to now, only a fraction of the work [49], [62] has annotated some evident causal relationships, and no complete causal-labeled dataset has yet appeared, which significantly dampens researchers' enthusiasm for Indefinite Data.

IV. BASELINE MODEL

A. Fundamental Framework

Considering the latent confounders, the SCM is written as:

$$x_{m,j} = \sum_{x_{m,i} \in Pa(x_{m,j})} f_{m,ij} x_{m,i} + \sum_{l_{m,k} \in Ec(x_{m,j})} g_{m,kj} l_{m,k} + \epsilon_{x_{m,j}} \quad (1)$$

where $Pa(x_{m,j})$ represents the parent set of $x_{m,j}$, $Ec(x_{m,j})$ is the confounder set having effects on $x_{m,j}$, f and g denotes the causal strengths and confounding strength, respectively, ϵ represents the exogenous i.i.d., noise term, and K is the number of latent confounders. $x \in \mathbb{R}^{N \times D}$, $l \in \mathbb{R}^{K \times D}$, $\epsilon_{x_{s,j}} \in \mathbb{R}^{N \times D}$, $0 \leq i \neq j < N$, $0 \leq k < K$. The matrix form reads:

$$X = AX + BL + E \quad (2)$$

We design a couple of encoder and decoder to model the generating process of causal representation:

$$Encoder : W = f_1(X) \quad (3)$$

$$Decoder : \hat{X}^* = f_2(W(BL + E)) \quad (4)$$

where $f(\cdot)$ perform nonlinear transforms (neural network as GNN or MLP layers are popular choices) and W represent $(I - A)^{-1}$. Please note, $f_1(X)$ is an abbreviation of $f_1(X(BL + E)^{-1})$ as X consist of $BL + E$ w.r.t. W . Decoder can be written by a maximization of leg-evidence:

$$\frac{1}{M} \frac{1}{S} \sum_{m=1}^M \sum_{s=1}^S \log p(X_{s,m}) = \frac{1}{M} \frac{1}{S} \sum_{m=1}^M \sum_{s=1}^S \log \int p(X_{s,m}|W)p(W)dW \quad (5)$$

Continuing the theory of variational Bayes, we regard W as the latent variable in variational autoencoder (VAE) [63] and use variational posterior $q(W|X)$ to approximate the intractable posterior $p(W|X)$, thus the evidence lower bound (ELBO) reads:

$$\mathcal{L}_{ELBO}^{s,m} = -KL(q(W|X_{s,m})||p(W)) + E_{q(W|X_{s,m})}[\log p(X_{s,m}|W)] \quad (6)$$

For simplicity, we model the prior as the standard normal $p(W) = \mathcal{MN}_{N \times N}(0, I, I)$, which indicates that each causal strength $p(f_{ij}) = \mathcal{N}(0, 1)$. Note that even though the nodes are probably connected in a true graph, however, they are independent in prior.

In the causal view, our framework consists of two functions: a causal strength encoder: $\mathcal{X} \rightarrow \mathcal{G}$ and a causal representation decoder: $\mathcal{G} \rightarrow \hat{\mathcal{X}}$.

B. Estimation of Confounding Effect

We use $c_{m,j} = \sum_{l_{m,k}} g_{m,kj} l_{m,k}$ to describe the confounding effect on $\hat{x}_{m,j}$ and $C = BL$ to describe the corresponding matrix form. Inspired by [64], we proposed a estimation about C :

$$c_{m,j} = \frac{p(x_{m,j})p(L|x_{m,j})}{\sum_i^N p(x_{m,i})p(L|x_{m,i})} x_{m,j} \quad (7)$$

Equation 7 only works when the expectation $E_{p(X)}(X|L)$ is much greater than the expectation $E_{p(X)}(X|\epsilon)$. It collaborates the inductive bias that when confounding effects drastically exceed independent noise, X is approximately contributed by C rather than E . Therefore, the disentangled causal representation \hat{X} can be written as:

$$\hat{X} \approx \begin{cases} \hat{X}^* - C, & (E_{p(X)}(X|L) \gg E_{p(X)}(X|\epsilon)) \\ \hat{X}^*, & else \end{cases} \quad (8)$$

C. Explanation

1) *How to Extend to Multi-value Representation?*: Given the existence of deconfoundment, we can, without loss of generality, write the SCM as: $\hat{x}_j = \sum_{\hat{x}_i \in Pa(\hat{x}_j)} f_{ij} \hat{x}_i + \epsilon_{x_j}$, where the independence of ϵ ensures the Causation Condition. That is, we can directly recover the causal relationship from the causal representation \hat{x} . For instance, if we linearly make causal representations \hat{a} to fit \hat{b} with an learnable parameter k in a downstream task, and obtain the corresponding residuals: $\Sigma_{\hat{b}} = \hat{b} - k\hat{a}$, $\Sigma_{\hat{a}} = \hat{a} - \frac{1}{k}\hat{b}$. Then, different causal relations can be determined through the independence combination between residuals and representations:

- $\Sigma_{\hat{a}} \perp \hat{b}, \Sigma_{\hat{b}} \not\perp \hat{a} \Rightarrow \hat{b} \rightarrow \hat{a}$

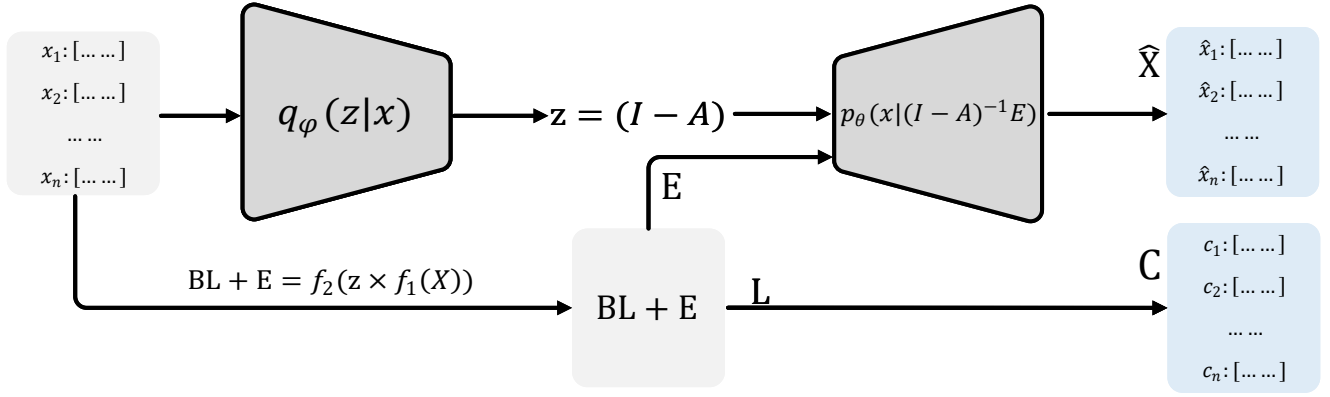


Fig. 1. An implementation example of our framework. $q_\varphi(z|\mathcal{X})$ predicts the causal strength from the input X . The predicted latent variable $z = (I - A)$, and then an causal representation decoder $p_\theta(x|(I - A)^{-1}E)$ learns to predict \hat{X} given the disentangled E and inverse of predicted z .

- $\Sigma_{\hat{a}} \not\perp \hat{b}, \Sigma_{\hat{b}} \perp \hat{a} \Rightarrow \hat{a} \rightarrow \hat{b}$
- $\Sigma_{\hat{a}} \not\perp \hat{b}, \Sigma_{\hat{b}} \not\perp \hat{a} \Rightarrow l \rightarrow \hat{a}, l \rightarrow \hat{b}$
- $\Sigma_{\hat{a}} \perp \hat{b}, \Sigma_{\hat{b}} \perp \hat{a} \Rightarrow \hat{a} \rightarrow l, \hat{b} \rightarrow l$

2) *How to Extend to Multi-structure Data?*: In contrast with popular methods that intuitively treat the noise matrix as a latent variable [18], [49] ($\mathcal{X} \rightarrow \mathcal{E}$ and $\mathcal{E} \rightarrow \hat{\mathcal{X}}$), we attempt to regard the causal strength as a latent variable, thereby enabling one model to learn multiple structures. From the overall view, sampling from a set of DAGs $\mathcal{G}_m = \{\mathcal{E}_m, \mathcal{V}_m\}_{m=1}^M$ is equal to generate a set of causal strengths which reads:

$$p(A) = \{p(A_m)\}_{m=1}^M \quad (9)$$

Moreover, to overcome the limitation that it is impossible to construct a loss function $loss(x, \hat{x})$ for multi-value representation, we map x and \hat{x} onto the space of Correlation relationships (see equation 21 for details). That is, x and \hat{x} remain consistent in the Correlation Condition, they conflict in the Causation Condition though.

D. Implementation Example

We formalized the dynamic variational inference model as follows: a causal strength encoder $f_\varphi : \mathcal{X} \rightarrow \mathcal{G}$, an causal representation decoder $f_\theta : \mathcal{G} \rightarrow \hat{\mathcal{X}}$, and an estimation function $f_\delta : \mathcal{X} \rightarrow \mathcal{C}$.

We resort to VAE to design the functions f_φ and f_θ as shown in Figure 1. Specifically,

1) *Encoder*: The encoder $q_\varphi(z|\mathcal{X})$ applies a graph attention module $f_{att,\varphi}$ [65] to the input. It produces an adjacent matrix across a lower triangular mask under Hypothesis 1.

$$q_\varphi(z|\mathcal{X}) = softmax(f_{att,\varphi}(X)) \quad (10)$$

The output z implies the possible distribution of causal strength over \mathcal{X} . Specifically, $z_{i,j} = 1$ indicates a high probability relation $x_j \rightarrow x_i$.

2) *Decoder*: we extract E by utilizing a multi-layer perceptron (MLP):

$$BL + E = GNN_{enc}(f_{att,\varphi}(X), X) \quad (11)$$

$$E = MLP_E(BL + E) \quad (12)$$

where GNN_{enc} is instantiated by graph neural network: $GNN(A, X) = eLU(A \times (X \times W))$, which yields a nonlinear multiple of adjacent matrix $A \in \mathbb{R}^{N \times N}$, feature matrix $X \in \mathbb{R}^{N \times D}$ and weight matrix $W \in \mathbb{R}^{D \times H}$, where H represents the dimensions of hidden layers. Then, the decoder accumulated the incoming messages to each node via causal strength z and employed a new graph neural network GNN_{dec} :

$$p_\theta(\hat{x}_c|z^{-1}E) = GNN_{dec}(z^{-1}, E) \quad (13)$$

The output of the decoder $\hat{x}_c \in \mathbb{R}^{N \times D}$ equals the dimension of \mathcal{X} and it is the pure causal representation of \hat{x} without confounding.

3) *Confounding Estimation*: We used the same MLP module to extract L and two sigmoid functions: $\sigma_{p(x_j)}(\cdot)$ and $\sigma_{p(L|x_j)}(\cdot)$, to project $p(x_j)$ and $p(L|x_j)$ into the range of $(0, 1)$, which expresses the probability estimating c_j .

$$L = MLP_L(BL + E) \quad (14)$$

$$c_j = \frac{\sigma_{p(x_j)}(x_j)\sigma_{p(L|x_j)}(L|x_j)}{\sum_i^N \sigma_{p(x_i)}(x_i)\sigma_{p(L|x_i)}(L|x_i)} x_j \quad (15)$$

The output $C \in \mathbb{R}^{N \times D}$ of Estimation module equals the individual-specific effects of confounding on each x_j if there exactly exists strong confounding.

4) *Reconstruction Error*: Given the contradiction between X and \hat{X} on the Causation Condition explained in Definition 1, we map the X and \hat{X} into the correlation space.

Moreover, considering the dynamics of confounding effects across samples (as shown in Equation 8), we naturally design a confounding score for each graph as $\omega(L) = rank(L)/N$ (L is computed by equation 15). The graphs with high $\omega(L)$ can be regarded as confounding samples because the high rank of the matrix $L \in \mathbb{R}^{N \times D}$ stands for the extensive independent terms in L , which indicates that sufficient exogenous confounding variables point to the X , and vice versa. Finally, the reconstruction error and ELBO can be encapsulated by:

$$l_{RC} = \omega(L)l_{rc}(X, \hat{X} + C) + (1 - \omega(L))l_{rc}(X, \hat{X}) \quad (16)$$

$$\mathcal{L} = l_{RC} - KL[q_\varphi(z|\mathcal{X})||p(z)] \quad (17)$$

Specifically, We adopt mean squared error (MSE) and cosine similarity in implementation:

$$l_{rc}(X, \hat{X}) = E_{q_\varphi(z|\mathcal{X})}[MSE(cs(X), cs(\hat{X}))] \quad (18)$$

$$l_{rc}(X, \hat{X} + C) = E_{q_\varphi(z|\mathcal{X})}[MSE(cs(X), cs(\hat{X} + C))] \quad (19)$$

$$cs(\cdot) = \sum_{0 \leq i < j < N} \text{cossim}(\cdot_i, \cdot_j) \quad (20)$$

$$(21)$$

V. NEW DATASETS

A. Causalogue

1) *Attributes*: *Causalogue* is the first dialogue dataset that includes comprehensive causal relationship labels for Indefinite data. Additionally, we employ GPT-4 generation as a substitute for data collection from the real world or manual simulation, which considerably mitigates the presence of obscure causal structures.

The dataset incorporates 10 types of causal structures (M = 10), each with several samples (Detailed numbers are presented in Table II, “Small” signifies samples that have been manually checked, while “large” refers to all samples generated by GPT-4 without manual verification). The detailed attributes are following:

Causal Variables: We treat each dialogue as a sample, comprised of 4 utterances, which we define as 4 causal variables. Further, the first and third utterances originate from the same speaker, defined as *speaker1*. Similarly, the second and fourth utterances are from another individual, defined as *speaker2*.

Causal Relationship: In each sample, binary causal relationships have been labeled between any two utterances—“1” represents that there exists a causal relationship and “0” represents there not.

Structure: We have designed 10 types of causal structures in the dataset as shown in Figure 2. Taking the Chain_II as an example, this model adds an additional causal relationship from $Utt_1 \rightarrow Utt_3$ based on the Chain_I, indicating that Utt_3 considers not just the effect from Utt_2 but also from Utt_1 .

Sample: We consider a dialogue as a sample, with each sample comprising 4 utterances representing 4 causal variables. Each sample corresponds to one of the 10 causal structures outlined above, annotating whether a causal relationship exists between any two utterances. Due to Hypothesis 1, our labels only consider forward-causal relationships. An example of a Chain_III sample is shown as follows:

“causal_type”: “Chain_III”,

“clause”: {“1”: “Your bill is 19.”, “2”: “Before I pay the bill, I have to express my dissatisfaction with the service I received tonight.”, “3”: “I’m so sorry to hear that but I don’t know what happened.”, “4”: “Specifically, It’s understandable to feel frustrated when something unexpected happens like spilling red wine on your clothes.”},

“dia_id”: 1,

“label”: {“1”: “0,0,0,0”, “2”: “1,0,0,0”, “3”: “0,1,0,0”, “4”: “0,1,1,0”}

In the given example, the Utt_4 serves as a response to the Utt_3 , while simultaneously attach to the speaker’s

Utt_2 —thereby rendering both the Utt_2 and Utt_3 as causes to the Utt_4 . Indeed, during the generation process of the Utt_4 , we made sure to inform GPT-4 of the existence of Utt_2 and Utt_3 .

2) *Creation Process*: We utilized the API interface of GPT-4¹ to defined the following variables: “role”, which has three types - “system”, “user”, and “assistant”. Here, “system” represents the background or a prior settings, while “user” and “assistant” are defined as speakers with two different identities. Additionally, the first utterance is pre-set. Hence, creating a dialogue requires a given combination: a fixed *first_utterance*, a specified *system* information, and a setting which previous utterances are considered. We have a total of 149 *first_utterance* options, and there are as many as 278,867 combinations of *first_utterance* and *system* settings (our final samples only number in the 1638, to preserve the diversity and distinctiveness of our dialogues). What follows is an example of generating the third utterance in the structure of ChainII:

{“role”: “system”, “content”: “You are Peter, you have promised to go to a Chinese Opera with your daughter, so you want to have dinner with your friends in next Sunday.” }

{“role”: “assistant”, “content”: “Yes. Sunday sounds fine. What time?” (pre-set Utt_1)}

{“role”: “user”, “content”: Utt_2 }

Upon creation, the samples are initially auto-annotated based on their designed labels, and then manually verified to ensure their validity. Our manual verification employed two annotators, who demonstrated proficient English understanding and communication skills, possessing sufficient knowledge about causality. The annotation consistency between these two annotators was tested through 833 samples, achieving a kappa coefficient of 0.92.

During the annotation process, if a sample was labelled differently by the two annotators, that sample was considered to possess an ambiguous causal relationship and thus was excluded from the final dataset. Only samples that were consistently labeled by both annotators were ultimately accepted.

Furthermore, to guarantee the freedom of manual annotation, we allowed the annotators to label structures that fell outside the predefined 10 causal structures. Specifically, we only requested annotators to judge whether any two utterances (satisfying Hypothesis 1) have a causal relationship, allowing them some discretion, which inevitably produced samples not belonging to the 10 causal structures. We classified these as the “Other” category.

The accuracy of labels was significantly improved after the manual annotation process. However, considering that the unverified samples might be utilized for other research areas, such as the ability of LLMs to focus on context, we have released two versions of the datasets, as demonstrated in Table II. “Small” signifies samples that have been manually checked as correctly labeled, while “large” refers to all samples generated by GPT-4 without manual verification. We do not recommend considering the “large” version when undertaking causality-related work. Likewise, we have not taken it into our experiments.

¹<https://platform.openai.com/docs/models/gpt-4>

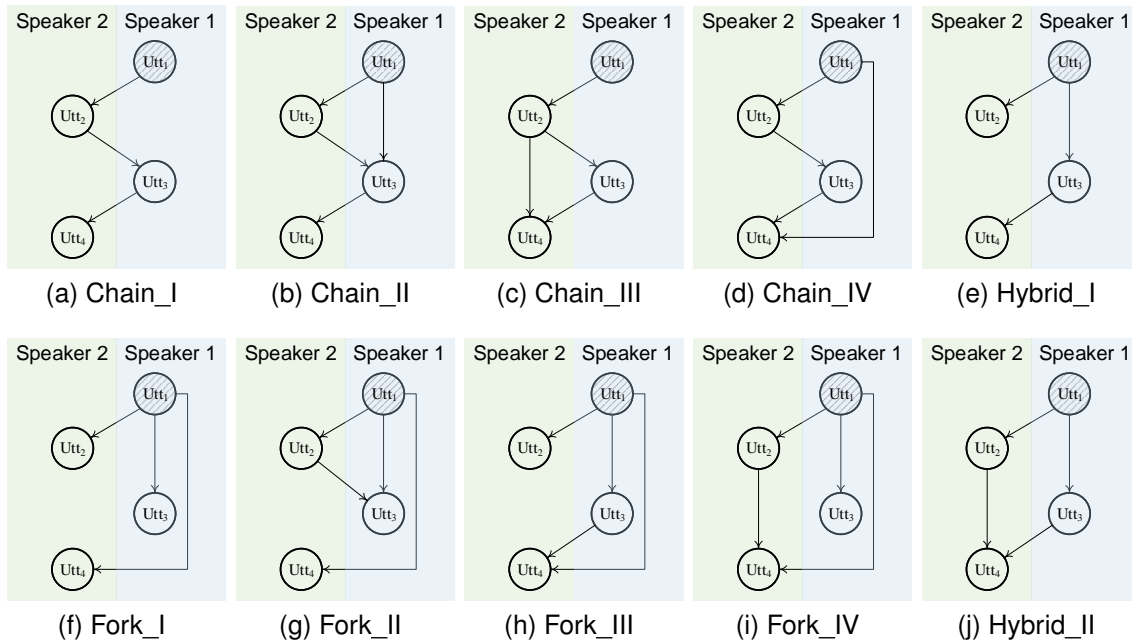


Fig. 2. 10 structures in *Causalogue* Dataset.

TABLE II
NUMBER OF THE SAMPLES IN *Causalogue* DATASET

Versions	Structure Types										Total
	Chain_I	Chain_II	Chain_III	Chain_IV	Fork_I	Fork_II	Fork_III	Fork_IV	Hybrid_I	Hybrid_II	
Small	276	84	141	44	257	237	251	67	185	77	1638
Large	0	524	508	513	1215	645	501	372	499	635	5412

B. Causaction

1) *Attributes*: *Causaction* is another Indefinite Dataset that we obtained after re-annotating the Breakfast Dataset [66]. It contains a total of 1,118 videos, documenting 10 different breakfast preparation processes (such as coffee, salad, sandwich, etc.). Each video consists of 4-9 actions, with a clear frame boundary. We have annotated the causal relationship between any two actions in a sample. Specific attributes are as follows:

Causal Variable: We treat each video as a sample, comprised of 4-9 actions as the causal variables. For simplicity, we follow the setting of MS-TCN [67], replacing the video resource of each action with pre-trained representation of I3D [68].

Causal Relationship: According to the Hypothesis 1, we deem the time order of these actions in certain video as natural linear order. Hence, binary causal relationships have been labeled between any two actions satisfying the linear order ('0' represents there is no causal relationship while '1' represents there is). For example, process "cereals" includes 4 actions: "take bowl", "pour cereals", "pour milk", and "stir cereals". The all causal relationships labeled with "1" are: "take bowl → pour cereals", "take bowl → pour milk", "take bowl → stir cereals", "pour cereals → stir cereals", and "pour milk → stir cereals".

Structure: Unlike *Causalogue*, although the entire dataset includes the 10 types of preparation processes of breakfasts, the number of causal structures far exceeds 10. Most videos do not encompass all the actions in a process. For example, the entire process of "Salad" consists of 7 actions, but some videos are missing the "take plate" action, and some videos include the actions "cut fruit1" and "cut fruit 2".

Sample: We consider a video as a sample. The statistics of samples with different processes are shown as Table III.

2) *Creation Process*: The original Breakfast Dataset, has annotated the frame boundaries of each action. Therefore, in our annotation work, we don't need to ascertain which frames a causal variable contains. The annotators were asked to directly annotate at the action level to avoid inconsistencies caused by the subjectivity of watching videos. For example, in the coffee process, there are 6 actions, so a total of 15 binary relationship pairs need to be annotated. Specifically, we informed the annotators of the time order and the explanation of all actions in each process. After ensuring the understanding of each action, the annotators conducted a causal relationship evaluation on binary action pairs (A, B) that satisfy the linear order relation, where 1 signifies a belief that action A has a causal relationship with action B , and 0 represents no such relationship. An action pair is considered to have a causal relationship if the following conditions are met:

TABLE III
THE NUMBER OF SAMPLES IN *Causaction* DATASET

Process	Number of Actions (Variables)						
	4	5	6	7	8	9	all
cereals	36	-	-	-	-	-	36
coffee	12	28	-	-	-	-	40
friedegg	52	45	53	7	4	-	161
milk	56	14	4	-	-	-	74
salad	6	52	29	25	37	33	182
sandwich	52	11	6	2	4	-	75
tea	14	5	-	-	-	-	19
pancake	-	100	26	24	33	41	224
scrambledegg	8	36	30	42	33	24	173
juice	65	36	24	6	-	3	134
all	301	327	172	106	111	101	1118

- According to life experience, after action A happens, action B is high-probably to occur.
- According to life experience, after action B happens, action A is low-probably to occur.

Finally, we binarize all annotation results, that is, binary pairs with a mean > 0.5 are marked as 1, and those with a mean < 0.5 are marked as 0.

The annotators consist of 10 researchers in the field of causal inference (Group A) and 217 deep-learning researchers (Group B). Initially, we asked Group A to annotate the two simplest processes, “milk” and “coffee,” and considered their annotation results as the gold standard. Members of Group B first annotated “milk” and “coffee,” with only those members having $> 80\%$ consistency with Group A deemed qualified. In the end, 190 qualified members were confirmed in Group B, joining the 10 members in Group A to form Group C (total 200 members). Group C annotated the remaining 8 processes, and the statistical results after binarization were used as the final labels. During the annotation process, the consistency was 94.13% for Group A, 88.46% for the qualified members of Group B, and 88.74% for Group C.

C. Task Definition

Followed by Definition 3, the causal variable $x_{s,m,n}$ is the n^{th} variable of a sample $X_{s,m} = (x_{s,m,1}, x_{s,m,2}, \dots, x_{s,m,N})$. The causal pair $(x_{s,m,i}, x_{s,m,j})$ ($x_{s,m,i} \preceq_{X_{s,m}} x_{s,m,j}$) represents the causal relationship from $x_{s,m,j}$ to $x_{s,m,i}$, and the causal representation $\hat{x}_{s,m,i}$ represents the learned-well deep representation meeting the Definition 1.

Thus, in a given sample, the fundamental task of Indefinite Data is to **extract all causal pairs** and **output causal representation** $\hat{X}_{s,m} = (\hat{x}_{s,m,1}, \hat{x}_{s,m,2}, \dots, \hat{x}_{s,m,N})$.

VI. EXPERIMENTS

Indefinite Data is regarded as a task that outputs both causal structures and causal representations, for which we have separately evaluated causal structures and causal representations. Considering that our baseline model has a disentanglement extension, we have additionally designed a synthetic dataset to analyze the ability to estimate the effects of confounding.

A. Existing Approaches and Details of Implementation

To the best of our knowledge, no existing approach can be applicable in Indefinite data. So we choose the SOTA work in Causal Discovery from multi-structure data and multi-value representation, respectively.

In multi-structure data, we evaluate our model with ACD [22] and AVICI [20]. In multi-value representation, we evaluate our model with CAE [49], CVAE [31], and DAG-GNN [18]. Meanwhile, for the disentanglement, we evaluate our model with some SOTA work focusing on latent confounders: **pcss** [64], **LFCM** [8], and **GIN** [69]. In the experiment, we made some necessary modifications to these methods to adapt them to Indefinite Data. For example, for ACD and AVICI, we increased the dimensions of the hidden layers to enlarge the representation space, while mapping the reconstruction loss into the correlation relationship space. For those methods focusing on multi-value data, we replaced the latent variables with causal strength.

In our Experiments, we utilized RoBERTa-base² as our pre-trained model for generating word embeddings in the *Causalogue*. Throughout the training process, a learning rate of 1e-5 was set, with the batch size and epochs set to 16 and 50, respectively. The dimension of the hidden layers within the network was also set to 768. For the *Causaction*, we use less batch size with 4 to overcome the variable length and adopt more dimensions of the hidden layers (1024) to match the more complex information in video representation. The entire training procedure was conducted on a NVIDIA GEFORCE 970 RTX 3090 graphics processing unit. In both datasets, the 100 samples were randomly selected for valid set and 200 samples were randomly selected for test set. Each result is evaluated by 10-fold cross-validation.

B. Causal Structure

We evaluated the performance of recovering causal structures (causal graphs) on *Causalogue* and *Causaction*, using 3 different metrics: area under a receiver operating characteristic (AUROC), mean Squared error (MSE), and Hamming distance (HD).

Table IV shows that our baseline model significantly outperforms existing methods with the applied necessary modifications. We believe this is due to the excessive specific assumptions made by existing methods for certain forms of data, which hinder their extension to a broader range of data forms. For instance, with DAG-GNN, even though we modified latent variables to adapt to Indefinite Data, with the acyclic constraint from NOTEARS [42], a unique phenomenon emerges during the optimization process: the adjacency matrix A tends to make A_{ij} and A_{ji} identical. This is advantageous for traditional causal data with unknown causal order, but conflicts with the linear order in Indefinite Data. Moreover, we found that methods for multi-structured data (ACD and AVICI) perform only second best to our method. This confirms that structure and representation are two individual aspects: multi-structure data have common laws, regardless of whether they are in single- or multi-value representation.

²<https://huggingface.co/roberta-base>

TABLE IV
PERFORMANCE OF RECOVERING CAUSAL GRAPHS, 95% CONFIDENCE INTERVAL SHOWN.

Method	<i>Causalogue</i>			<i>Causaction</i>		
	AUROC	MSE	HD	AUROC	MSE	HD
ACD	0.55±0.024	0.31±0.005	0.82±0.018	0.65±0.011	0.41±0.013	1.4±0.023
AVICI	0.57±0.019	0.37±0.003	0.86±0.024	0.69±0.009	0.44±0.011	1.2±0.016
CAE	0.54±0.021	0.41±0.005	0.79±0.021	0.61±0.012	0.48±0.012	1.3±0.019
CVAE	0.56±0.014	0.40±0.001	0.88±0.013	0.59±0.011	0.51±0.015	1.6±0.021
DAG-GNN	0.41±0.034	0.36±0.003	0.78±0.015	0.59±0.007	0.45±0.009	1.8±0.020
Ours	0.69 ±0.019	0.26 ±0.002	0.49 ±0.019	0.78 ±0.008	0.30 ±0.009	1.1 ±0.023

TABLE V
PERFORMANCE OF RECOVERING CAUSAL GRAPHS OUT OF DISTRIBUTION

Method	<i>Causalogue</i>			<i>Causaction</i>		
	AUROC	MSE	HD	AUROC	MSE	HD
ACD	0.51±0.031	0.46±0.025	1.63±0.049	0.53±0.034	0.58±0.028	2.1±0.046
AVICI	0.51±0.045	0.46±0.032	1.13±0.051	0.60±0.049	0.54±0.037	2.8±0.041
CAE	0.46±0.033	0.46±0.035	1.37±0.054	0.61±0.035	0.63±0.039	2.5±0.055
CVAE	0.49±0.044	0.48±0.028	1.37±0.046	0.52±0.039	0.49±0.045	2.9±0.048
DAG-GNN	0.33±0.041	0.43±0.029	1.45±0.049	0.48±0.044	0.53±0.039	2.7±0.043
Ours	0.61 ±0.024	0.35 ±0.008	0.94 ±0.027	0.66 ±0.016	0.42 ±0.014	1.8 ±0.031

In addition, the ability to generalize out of distributions is essential for multi-structure data. To test whether these models can maintain robustness when encountering new causal structures, we designed a simple 10-fold experiment. In each fold, we randomly selected 2 structures (of *Causalogue*) or processes (of *Causaction*) for the test set, with all its samples prohibited from appearing in the train and valid sets.

Table V records the results of the cross-distribution test-set. Our method consistently outperforms existing methods, and the entire statistical result shows a situation similar to that of Table IV. Additionally, we noticed that the standard deviation of our method is much lower than other methods. We consider that for the reason there are similarities among some structures in the dataset. For instance, in the *Causalogue* dataset, Hybrid_II is very similar to Hybrid_I, but significantly different from the other 8 structures. In the *Causaction* dataset, many common causal relationships exist among “friedegg” and “pancake”. When these structures are chosen for the test set in certain folds, the model can find “answers” from similar structures in the train set. However, when similar structures are all present in the test set fold (e.g., the test set includes Hybrid_I and Hybrid_II), it is difficult for the trained structures to manifest apparent invariance. However, the lowest standard deviation once-again demonstrated the superiority of our baseline in releasing many assumptions about data forms. In other words, existing methods tend to rely on specific hypotheses to recover causal relationships, while our approach is more inclined to let the model itself learn the causal relationships.

C. Causal Representation

Evaluating causal representation is another crucial aspect of Indefinite Data. According to Definition 1, causal representa-

tion needs to be evaluated on both correlation and causation. Specifically, we assume x_i and x_j to be any two causal representations that need to be tested. We propose a correlation matrix, Cor , to verify the performance in correlation, where $Cor_{ij} = \text{cossin}(x_i, x_j)$. Moreover, we train a downstream linear layer to extract causal relationships, $Cas_{ij} = \text{linearlayer}(x_i || x_j)$. Both Cor and Cas are evaluated by AUROC and MSE, to demonstrate the performance of the causal representation in correlation and causation, respectively.

Table VI presents the performance in correlation and causation. The results suggest that the representation more easily grasps the information of correlation, while causation, an asymmetric and underlying relation, poses a more challenging topic in representation learning. Moreover, our method significantly outperforms others, even when we have modified them to adapt multi-value representations. This reason aligns with Section VI-B, for instance, the causality in ACD is based on the Granger causality hypothesis in time series, which stresses the faithfulness of single clues to causation. However, when it is expanded to other types of data (like the current Indefinite Data), it is tough to ascertain the correct set of parent nodes for causal representation. In addition, similar to the performance of causal structure, methods of multivalued representation (CAE, CVAE, DAG-GNN) also show superior performance in Table VI over the multi-structure data methods. Thus, we can emphasize that representation and structure are two separate dimensions, and the concurrent existence of multi-value representation and multi-structure data leads to new challenges.

D. Disentanglement

We created a set of synthetic dataset to evaluate the estimation of confounding effects. Specifically, We randomly draw

TABLE VI
PERFORMANCE OF LEARNING CAUSAL REPRESENTATIONS

Method	<i>Causalogue</i>				<i>Causaction</i>			
	<i>Cas</i>		<i>Cor</i>		<i>Cas</i>		<i>Cor</i>	
	AUROC	MSE	AUROC	MSE	AUROC	MSE	AUROC	MSE
ACD	0.52 ±0.026	0.64 ±0.074	0.91 ±0.013	0.43 ±0.022	0.59±0.006	0.39 ±0.009	0.88 ±0.001	0.28 ±0.005
AVICI	0.57 ±0.021	0.59 ±0.032	0.91 ±0.017	0.31 ±0.016	0.62 ±0.002	0.34 ±0.009	0.94±0.001	0.21 ±0.001
CAE	0.61 ±0.023	0.52 ±0.047	0.93 ±0.011	0.32 ±0.013	0.64 ±0.001	0.36 ±0.011	0.92 ±0.003	0.25 ±0.003
CVAE	0.62 ±0.021	0.55 ±0.066	0.91 ±0.006	0.29 ±0.024	0.61 ±0.005	0.31 ±0.005	0.92±0.001	0.23 ±0.003
DAG-GNN	0.59 ±0.019	0.55 ±0.059	0.90 ±0.017	0.39 ±0.009	0.63 ±0.003	0.33±0.013	0.91 ±0.002	0.26 ±0.002
Ours	0.68 ±0.016	0.43 ±0.058	0.95 ±0.008	0.26 ±0.011	0.79 ±0.005	0.26 ±0.004	0.96 ±0.002	0.15 ±0.001

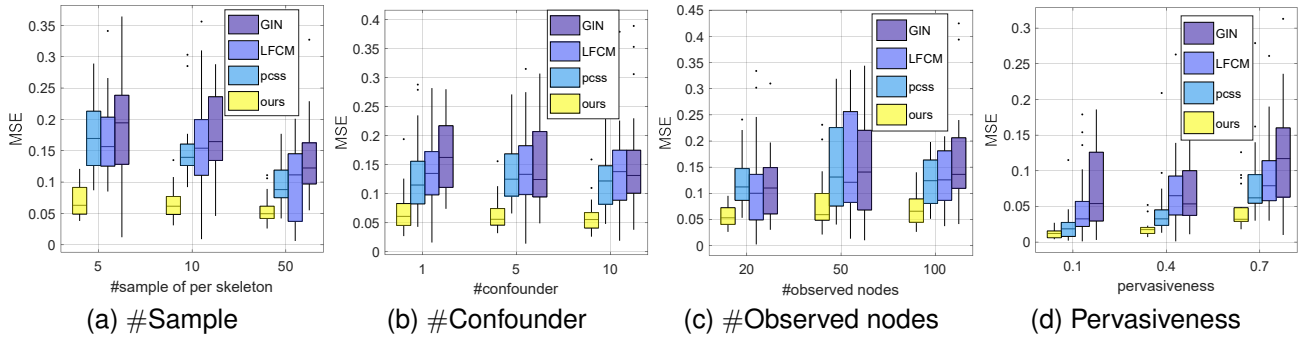


Fig. 3. MSE error across all ingredients setting for estimating C via GIN, LFCM, pcss, and ours.

Causal DAG from a random graph model with an expected neighborhood size of 5 and consider graphs with the number of observed nodes $N \in \{20, 50, 100\}$. For probing how our approach is affected by the pervasiveness of confounding, we assume that each confounder l_k is a direct cause of node x_i with a chance $P \in \{0.1, 0.4, 0.7\}$. Given the graph, we stochastically set a trend type for each causal strength weight with equal probability. Meanwhile, we add $N(0, \sigma_{noise}^2)$ noise to each node. Finally, we consider the number of confounders $K \in \{1, 5, 10\}$ and the number of samples of each skeleton $n \in \{5, 10, 50\}$, respectively.

In Figure 3, we quantify the mean-squared estimation (MSE) error of C . Our method likewise performs best in all ingredient settings, demonstrating that our confounding disentanglement pool the statistical strength better than other estimation algorithms in multi skeleton data. Besides, combined with the conclusion in [64], this error should decrease as the number of samples n increases. Figure 3 (a) is exactly indicative of this conclusion.

VII. DISCUSSION

This paper focuses on causal inference for a novel paradigm of data - Indefinite Data, characterized by multi-structure data and multi-value representations. These two features differ greatly from traditional experimental data, thereby causing existing methods to be non-adaptive to Indefinite Data. To provide a good starting point for causal research on Indefinite Data, we introduce two brand new datasets- *Causalogue* and *Causaction*, analyze the challenges brought about by the coexistence of multi-structure data and multi-value representations,

and propose a corresponding probabilistic framework. In the experiments, we exhibit benchmark results for both structure and representation and share intrinsic insights in the extension of disentanglement.

However, such a probabilistic framework is inconsistent for the learning of causal structure and causal representation. Specifically, for multi-structure scenarios, learned causal strength $\hat{f} = h_1(X, \varphi)$ (φ represents the parameters of encoder), and for multi-value representation, $\hat{X} = h_2(X, \hat{f})$. And $D > 1$ makes $loss(\hat{X}, X)$ be replaced with $loss(cs(\hat{X}), cs(X))$. Therefore, when only $loss(\hat{f}, f)$ exists, we can get $\hat{f} = f$ and $f \Leftrightarrow X$. However, we cannot guarantee $\hat{X} \Leftrightarrow \hat{f}$ for $X = \hat{X}$, thus severe inconsistencies exist. This phenomenon doesn't exist in other data paradigms, For instance, when $M = 1 \& D > 1$, we can guarantee $\hat{f} \Leftrightarrow \hat{X}$, and thus ensure $X = \hat{X}$ by a fixed causal structure. Meanwhile, when $M > 1 \& D = 1$, $\hat{f} = f \Leftrightarrow X = \hat{X}$ can be achieved through $loss(\hat{X}, X)$ and $loss(\hat{f}, f)$. We have elaborated on this problem and proposed an intervention-based improvement in our latest work [70].

Causal research on Indefinite Data will be a long-term topic. The ultimate goal of multi-structure data is to exhibit cross-distribution learning capability, while multi-value representations will eventually rely on a model-driven learning process. In previous work, we posited such a challenge, and this paper makes it feasible from a set of research basis. We hope this will attract an increasing number of researchers to contribute to the growing body of work applying causal inference to the real world.

REFERENCES

- [1] C. T. Jerzak, F. Johansson, and A. Daoud, "Image-based treatment effect heterogeneity," *arXiv preprint arXiv:2206.06417*, 2022.
- [2] F. D. S. Ribeiro, T. Xia, M. Monteiro, N. Pawlowski, and B. Glocker, "High fidelity image counterfactuals with probabilistic causal models," 2023.
- [3] W. Zhang, T. Wu, Y. Wang, Y. Cai, and H. Cai, "Towards trustworthy explanation: On causal rationalization," *arXiv preprint arXiv:2306.14115*, 2023.
- [4] S. S. G. Bagi, Z. Gharraee, O. Schulte, and M. Crowley, "Generative causal representation learning for out-of-distribution motion forecasting," *arXiv preprint arXiv:2302.08635*, 2023.
- [5] S. Sun, S. Zhi, Q. Liao, J. Heikkilä, and L. Liu, "Unbiased scene graph generation via two-stage causal modeling," *IEEE Transactions on Pattern Analysis and Machine Intelligence*, vol. 45, no. 10, pp. 12 562–12 580, 2023.
- [6] Z. Li, R. Cai, T. Z. J. Fu, Z. Hao, and K. Zhang, "Transferable time-series forecasting under causal conditional shift," *IEEE Transactions on Pattern Analysis and Machine Intelligence*, pp. 1–18, 2023.
- [7] A. Golan and D. K. Foley, "Understanding the constraints in maximum entropy methods for modeling and inference," *IEEE Transactions on Pattern Analysis and Machine Intelligence*, vol. 45, no. 3, pp. 3994–3998, 2023.
- [8] C. Squires, A. Yun, E. Nichani, R. Agrawal, and C. Uhler, "Causal structure discovery between clusters of nodes induced by latent factors," in *Conference on Causal Learning and Reasoning*. PMLR, 2022, pp. 669–687.
- [9] K. Zhang, B. Huang, J. Zhang, C. Glymour, and B. Schölkopf, "Causal discovery from nonstationary/heterogeneous data: Skeleton estimation and orientation determination," in *IJCAI: Proceedings of the Conference*, vol. 2017. NIH Public Access, 2017, p. 1347.
- [10] W. Wang, J. Gao, and C. Xu, "Weakly-supervised video object grounding via causal intervention," *IEEE Transactions on Pattern Analysis and Machine Intelligence*, vol. 45, no. 3, pp. 3933–3948, 2023.
- [11] K. Olesen, "Causal probabilistic networks with both discrete and continuous variables," *IEEE Transactions on Pattern Analysis and Machine Intelligence*, vol. 15, no. 3, pp. 275–279, 1993.
- [12] C. Xu, C. Liu, X. Sun, S. Yang, Y. Wang, C. Wang, and Y. Fu, "Patchmix augmentation to identify causal features in few-shot learning," *IEEE Transactions on Pattern Analysis and Machine Intelligence*, vol. 45, no. 6, pp. 7639–7653, 2023.
- [13] K. Li and Y. Fu, "Prediction of human activity by discovering temporal sequence patterns," *IEEE Transactions on Pattern Analysis and Machine Intelligence*, vol. 36, no. 8, pp. 1644–1657, 2014.
- [14] Y. Liu, G. Li, and L. Lin, "Cross-modal causal relational reasoning for event-level visual question answering," *IEEE Transactions on Pattern Analysis and Machine Intelligence*, vol. 45, no. 10, pp. 11 624–11 641, 2023.
- [15] A. Balashankar and L. Subramanian, "Learning faithful representations of causal graphs," in *Proceedings of the 59th Annual Meeting of the Association for Computational Linguistics and the 11th International Joint Conference on Natural Language Processing (Volume 1: Long Papers)*, 2021, pp. 839–850.
- [16] H. Chen, K. Du, C. Li, and X. Yang, "A review and roadmap of deep causal model from different causal structures and representations," *arXiv preprint arXiv:2311.00923*, 2023.
- [17] J. Pearl *et al.*, "Models, reasoning and inference," *Cambridge, UK: CambridgeUniversityPress*, vol. 19, no. 2, 2000.
- [18] Y. Yu, J. Chen, T. Gao, and M. Yu, "Dag-gnn: Dag structure learning with graph neural networks," in *International Conference on Machine Learning*. PMLR, 2019, pp. 7154–7163.
- [19] S. Lachapelle, P. Brouillard, T. Deleu, and S. Lacoste-Julien, "Gradient-based neural dag learning," *arXiv preprint arXiv:1906.02226*, 2019.
- [20] L. Lorch, S. Sussex, J. Rothfuss, A. Krause, and B. Schölkopf, "Amortized inference for causal structure learning," *Advances in Neural Information Processing Systems*, vol. 35, pp. 13 104–13 118, 2022.
- [21] N. R. Ke, J. X. Wang, J. Mitrovic, M. Szummer, and D. J. Rezende, "Amortized learning of neural causal representations," *stat*, vol. 1050, p. 21, 2020.
- [22] S. Löwe, D. Madras, R. Zemel, and M. Welling, "Amortized causal discovery: Learning to infer causal graphs from time-series data," in *Conference on Causal Learning and Reasoning*. PMLR, 2022, pp. 509–525.
- [23] S. M. Smith, K. L. Miller, G. Salimi-Khorshidi, M. Webster, C. F. Beckmann, T. E. Nichols, J. D. Ramsey, and M. W. Woolrich, "Network modelling methods for fmri," *Neuroimage*, vol. 54, no. 2, pp. 875–891, 2011.
- [24] W. Zhou, S. Yu, and B. Chen, "Causality detection with matrix-based transfer entropy," *Information Sciences*, vol. 613, pp. 357–375, 2022.
- [25] R. Cai, F. Xie, C. Glymour, Z. Hao, and K. Zhang, "Triad constraints for learning causal structure of latent variables," *Advances in neural information processing systems*, vol. 32, 2019.
- [26] A. Tank, I. Covert, N. Foti, A. Shojaie, and E. B. Fox, "Neural granger causality," *IEEE Transactions on Pattern Analysis and Machine Intelligence*, vol. 44, no. 8, pp. 4267–4279, 2022.
- [27] Z. Li, Q. Li, X. Zou, and J. Ren, "Causality extraction based on self-attentive bilstm-crf with transferred embeddings," *Neurocomputing*, vol. 423, pp. 207–219, 2021.
- [28] H. Zhang, L. Xiao, X. Cao, and H. Foroosh, "Multiple adverse weather conditions adaptation for object detection via causal intervention," *IEEE Transactions on Pattern Analysis and Machine Intelligence*, pp. 1–1, 2022.
- [29] G. Oh, E. Jeong, and S. Lim, "Causal affect prediction model using a facial image sequence," *arXiv preprint arXiv:2107.03886*, 2021.
- [30] H. Guvenir, B. Acar, G. Demiroz, and A. Cekin, "A supervised machine learning algorithm for arrhythmia analysis," in *Computers in Cardiology 1997*, 1997, pp. 433–436.
- [31] H. Chen, B. Liao, J. Luo, W. Zhu, and X. Yang, "Learning a structural causal model for intuition reasoning in conversation," 2023.
- [32] K. Du, X. Yang, and H. Chen, "Casr: Refining action segmentation via marginalizing frame-level causal relationships," 2023.
- [33] J. Li, B. Wu, X. Sun, and Y. Wang, "Causal hidden markov model for time series disease forecasting," in *Proceedings of the IEEE/CVF Conference on Computer Vision and Pattern Recognition*, 2021, pp. 12 105–12 114.
- [34] Y. Xia, Y. Liang, H. Wen, X. Liu, K. Wang, Z. Zhou, and R. Zimmermann, "Deciphering spatio-temporal graph forecasting: A causal lens and treatment," in *Thirty-seventh Conference on Neural Information Processing Systems*, 2023.
- [35] Y. Zhao, P. Deng, J. Liu, X. Jia, and J. Zhang, "Generative causal interpretation model for spatio-temporal representation learning," in *Proceedings of the 29th ACM SIGKDD Conference on Knowledge Discovery and Data Mining*, 2023, pp. 3537–3548.
- [36] S. Varambally, Y.-A. Ma, and R. Yu, "Discovering mixtures of structural causal models from time series data," *arXiv preprint arXiv:2310.06312*, 2023.
- [37] G. D'Acunto, G. D. F. Morales, P. Bajardi, and F. Bonchi, "Learning multiscale non-stationary causal structures," *Transactions on Machine Learning Research*, 2023.
- [38] Q.-D. Tran, P. Nguyen, B. Duong, and T. Nguyen, "Topological ordering in differentiable bayesian structure learning with guaranteed acyclicity constraint," *arXiv preprint arXiv:2309.01392*, 2023.
- [39] S. Fan, X. Wang, Y. Mo, C. Shi, and J. Tang, "Debiasing graph neural networks via learning disentangled causal substructure," *arXiv preprint arXiv:2209.14107*, 2022.
- [40] Y. Li, A. Torralba, A. Anandkumar, D. Fox, and A. Garg, "Causal discovery in physical systems from videos," *Advances in Neural Information Processing Systems*, vol. 33, pp. 9180–9192, 2020.
- [41] C. Busso, M. Bulut, C.-C. Lee, A. Kazemzadeh, E. Mower, S. Kim, J. N. Chang, S. Lee, and S. S. Narayanan, "Iemocap: Interactive emotional dyadic motion capture database," *Language resources and evaluation*, vol. 42, no. 4, pp. 335–359, 2008.
- [42] X. Zheng, B. Aragam, P. K. Ravikumar, and E. P. Xing, "Dags with no tears: Continuous optimization for structure learning," *Advances in neural information processing systems*, vol. 31, 2018.
- [43] D. Lopez-Paz, R. Nishihara, S. Chintala, B. Schölkopf, and L. Bottou, "Discovering causal signals in images," in *Proceedings of the IEEE conference on computer vision and pattern recognition*, 2017, pp. 6979–6987.
- [44] M. Shadaydeh, L. Müller, D. Schneider, M. Thümmel, T. Kessler, and J. Denzler, "Analyzing the direction of emotional influence in nonverbal dyadic communication: A facial-expression study," *IEEE Access*, vol. 9, pp. 73 780–73 790, 2021.
- [45] C. Mao, K. Xia, J. Wang, H. Wang, J. Yang, E. Bareinboim, and C. Vondrick, "Causal transportability for visual recognition," in *Proceedings of the IEEE/CVF Conference on Computer Vision and Pattern Recognition*, 2022, pp. 7521–7531.
- [46] I. Beltagy, K. Lo, and A. Cohan, "Scibert: A pretrained language model for scientific text," *arXiv preprint arXiv:1903.10676*, 2019.
- [47] S. Zhao, T. Liu, S. Zhao, Y. Chen, and J.-Y. Nie, "Event causality extraction based on connectives analysis," *Neurocomputing*, vol. 173, pp. 1943–1950, 2016.

- [48] C. S. Khoo, S. Chan, and Y. Niu, "Extracting causal knowledge from a medical database using graphical patterns," in *Proceedings of the 38th annual meeting of the association for computational linguistics*, 2000, pp. 336–343.
- [49] H. Chen, X. Yang, J. Luo, and W. Zhu, "How to enhance causal discrimination of utterances: A case on affective reasoning," in *Proceedings of the 2023 Conference on Empirical Methods in Natural Language Processing*, H. Bouamor, J. Pino, and K. Bali, Eds. Singapore: Association for Computational Linguistics, Dec. 2023, pp. 494–512. [Online]. Available: <https://aclanthology.org/2023.emnlp-main.33>
- [50] Y. Wu, X. Wang, A. Zhang, X. He, and T.-S. Chua, "Discovering invariant rationales for graph neural networks," in *International Conference on Learning Representations*, 2021.
- [51] A. Hazan, P. Brossier, R. Marxer, and H. Purwins, "What/when causal expectation modelling in monophonic pitched and percussive audio," in *NIPS music, brain and cognition workshop*. Whistler, CA, 2007.
- [52] X. Li, S. Xie, P. McColgan, S. J. Tabrizi, R. I. Scahill, D. Zeng, and Y. Wang, "Learning subject-specific directed acyclic graphs with mixed effects structural equation models from observational data," *Frontiers in genetics*, vol. 9, p. 430, 2018.
- [53] A. Dhir and C. M. Lee, "Integrating overlapping datasets using bivariate causal discovery," in *Proceedings of the AAAI Conference on Artificial Intelligence*, vol. 34, no. 04, 2020, pp. 3781–3790.
- [54] B. Huang, K. Zhang, J. Zhang, J. D. Ramsey, R. Sanchez-Romero, C. Glymour, and B. Schölkopf, "Causal discovery from heterogeneous/nonstationary data." *J. Mach. Learn. Res.*, vol. 21, no. 89, pp. 1–53, 2020.
- [55] B. Huang, K. Zhang, M. Gong, and C. Glymour, "Causal discovery from multiple data sets with non-identical variable sets," in *Proceedings of the AAAI Conference on Artificial Intelligence*, vol. 34, no. 06, 2020, pp. 10 153–10 161.
- [56] S. Roy and D. Roth, "Solving general arithmetic word problems," *arXiv preprint arXiv:1608.01413*, 2016.
- [57] A. Talmor, J. Herzig, N. Lourie, and J. Berant, "Commonsenseqa: A question answering challenge targeting commonsense knowledge," *arXiv preprint arXiv:1811.00937*, 2018.
- [58] J. Wei, X. Wang, D. Schuurmans, M. Bosma, F. Xia, E. Chi, Q. V. Le, D. Zhou *et al.*, "Chain-of-thought prompting elicits reasoning in large language models," *Advances in Neural Information Processing Systems*, vol. 35, pp. 24 824–24 837, 2022.
- [59] J. Lee, S. Kim, S. Kim, J. Park, and K. Sohn, "Context-aware emotion recognition networks," in *Proceedings of the IEEE/CVF international conference on computer vision*, 2019, pp. 10 143–10 152.
- [60] S. Stein and S. J. McKenna, "Combining embedded accelerometers with computer vision for recognizing food preparation activities," in *Proceedings of the 2013 ACM international joint conference on Pervasive and ubiquitous computing*, 2013, pp. 729–738.
- [61] Y. Li, H. Su, X. Shen, W. Li, Z. Cao, and S. Niu, "Dailydialog: A manually labelled multi-turn dialogue dataset," *arXiv preprint arXiv:1710.03957*, 2017.
- [62] S. Poria, N. Majumder, D. Hazarika, D. Ghosal, R. Bhardwaj, S. Y. B. Jian, P. Hong, R. Ghosh, A. Roy, N. Chhaya *et al.*, "Recognizing emotion cause in conversations," *Cognitive Computation*, vol. 13, no. 5, pp. 1317–1332, 2021.
- [63] D. P. Kingma and M. Welling, "Auto-encoding variational bayes," 2022.
- [64] R. Agrawal, C. Squires, N. Prasad, and C. Uhler, "The decamfounder: Non-linear causal discovery in the presence of hidden variables," *arXiv preprint arXiv:2102.07921*, 2021.
- [65] P. Veličković, G. Cucurull, A. Casanova, P. Lio, and Y. Bengio, "Graph attention networks," *arXiv preprint arXiv:1710.10903*, 2017.
- [66] H. Kuehne, A. Arslan, and T. Serre, "The language of actions: Recovering the syntax and semantics of goal-directed human activities," in *Proceedings of the IEEE conference on computer vision and pattern recognition*, 2014, pp. 780–787.
- [67] Y. A. Farha and J. Gall, "Ms-tcn: Multi-stage temporal convolutional network for action segmentation," in *Proceedings of the IEEE/CVF conference on computer vision and pattern recognition*, 2019, pp. 3575–3584.
- [68] J. Carreira and A. Zisserman, "Quo vadis, action recognition? a new model and the kinetics dataset," in *proceedings of the IEEE Conference on Computer Vision and Pattern Recognition*, 2017, pp. 6299–6308.
- [69] F. Xie, R. Cai, B. Huang, C. Glymour, Z. Hao, and K. Zhang, "Generalized independent noise condition for estimating latent variable causal graphs," *Advances in Neural Information Processing Systems*, vol. 33, pp. 14 891–14 902, 2020.
- [70] H. Chen, X. Yang, and K. Du, "Ssl framework for causal inconsistency between structures and representations," 2023.